



Science Arts & Métiers (SAM)

is an open access repository that collects the work of Arts et Métiers ParisTech researchers and makes it freely available over the web where possible.

This is an author-deposited version published in: <http://sam.ensam.eu>
Handle ID: <http://hdl.handle.net/10985/10321>

To cite this version :

Agathe NÉROT, Wafa SKALLI, Xuguang WANG - An assessment of the realism of digital human manikins used for simulation in ergonomics - Ergonomics p.13 - 2015

Any correspondence concerning this service should be sent to the repository

Administrator : archiveouverte@ensam.eu

An assessment of the realism of digital human manikins used for simulation in ergonomics

Agathe Nérot^{1,2,3,4}, Wafa Skalli⁴, Xuguang Wang^{1,2,3}

¹*Université de Lyon, F-69622 Lyon, France*

²*Université Claude Bernard Lyon 1, Villeurbanne*

³*IFSTTAR, UMR_T9406, LBMC Laboratoire de Biomécanique et Mécanique des Chocs, F69675, Bron*

⁴*LBM-Institut de Biomécanique Humaine Georges Charpak, Arts et Métiers ParisTech, 151, Boulevard de l'hôpital, 75013 Paris, France*

* Corresponding author: Xuguang Wang, IFSTTAR-LBMC, 25 av. F. Mitterrand, case 24, 69675 BRON Cedex, France

Tel: +33 (0)4.72.14.24.51

Fax: +33 (0)4.72.14.23.60

Email: xuguang.wang@ifsttar.fr

Abstract

In this study, the accuracy of the joint centers of the manikins generated by RAMSIS and Human Builder (HB), two digital human modeling systems widely used in industry for virtual ergonomics simulation, was investigated. Eighteen variously sized females and males were generated from external anthropometric dimensions and six joint centers (knee, hip and four spine joints) were compared with their anatomic locations obtained from the three-dimensional reconstructed bones from a low-dose X-ray system. Both RAMSIS and HB could correctly reproduce external anthropometric dimensions while the estimation of internal joint centers location presented an average error of 27.6mm for HB and 38.3mm for RAMSIS. Differences between both manikins showed that a more realistic kinematic linkage led to better accuracy in joint location. This study opens the way to further research on the relationship between the external body geometry and internal skeleton in order to improve the realism of the internal skeleton of digital human models especially for a biomechanical analysis requiring information of joint load and muscle force estimation.

Keywords

Digital Human Models; Anthropometry; Joint center, Stereo-radiography

Practitioner summary (50 words)

The present study assessed two digital human modeling systems widely used in industry for virtual ergonomics. Results support the need of a more realistic human modelling especially for a biomechanical analysis and a standardization of digital human models.

1. Introduction

Digital human models (DHM) have been developed since early 1960s and are now used by engineers for ergonomics assessment of a product or a workplace in its early phase of development (see an extensive review of DHMs by Bubb and Frizsche, 2009). They are mainly used for specifying spatial layout of a product/workplace such as vehicle interior and/or biomechanical assessment of workload through simulation of task related posture/motion of a target population. The human models behind these simulation tools are quite similar and composed of an external body shape and an internal articulated linkage representing the skeleton with more and less degrees of freedom (DOFs). More recently, more advanced human models have been developed for specific applications. For instance, a detailed musculoskeletal model is implemented in Anybody human modeling software, aiming to estimate muscles forces through inverse dynamics (Damsgaard et al., 2006). Muscle activation in a driving posture was simulated by Grujicic et al. (2010) using Anybody for assessing long-distance driving fatigue. In case of seating comfort simulation, even more sophisticated deformable finite elements models with a realistic representation of soft tissues in the buttock and thigh were developed in CASIMIR human model (Siefert and Pankoke, 2012). To investigate many issues raised for the design of a product like an automotive, different human models with different functionalities are often needed.

Accurately locating joint centers of these human models is important especially for biomechanical analysis of workload in manual material handling. Joint moments at critical joints such as L5/S1 and shoulder, need to be calculated at first and then compared with joint moment strength, as explained by Chaffin (1997) in case of developing “3D Static Strength Prediction Program” (3DSSPP). An inaccurate joint location will certainly lead to inaccuracy in joint load estimation. Accurately locating joint centers is also important when different human models need to be used together. For this, not only a common data exchange protocol is required as suggested by Bonin et al. (2014), but more importantly, human models should be anatomically correct with a realistic representation of joint centers. A same set of joint angles will lead to different postures in case of different joint centers for a same kinematic linkage. If the posture predicted by a multi-body model without muscles like RAMSIS is used as input for a musculoskeletal model like Anybody, one has to ensure that joint centers predicted by RAMSIS should be accurate enough because an error in joint location would highly affect muscle force estimation. For instance, Delp and Maloney (1993) showed that a 2

cm superior displacement of hip joint center decreased abduction moment arm by 12% and maximum isometric abduction moment by 49%.

However to our knowledge, few studies have been published verifying the realism of currently existing human models. Zehner et al. (2009) performed a validation and verification study of five DHMs for ergonomic assessment of the aircraft F-16D cockpit. Only a few external anthropometric dimensions were compared between generated digital manikins and real subjects without looking at internal joint location. Thanks to recent progress in medical imaging, data of both external body shape and internal skeleton is becoming available. For example, the low dose radiation EOS system is capable of extracting 3D external body shape and 3D bone envelop of the whole body from two simultaneous anterior-posterior and lateral X-rays (Dubousset et al., 2010). Therefore, this study aimed to verify how realistic existing digital human models are especially in terms of joint location. Two widely used DHMs were selected, Dassault Systèmes' Human Builder (HB) and Human Solutions' RAMSIS. The first is widely used in manufacturing process assessment with a full representation of thoracic and lumbar spines, while the second is mainly used for vehicle interior design with a more simplified spine model.

2. Materials and methods

2.1. Data acquisition

Eighteen subjects were selected from the database of both internal and external geometry of the human body described in Bertrand et al. (2006). The participants were healthy adults with a limited range of (Body Mass Index) BMI. Few participants had a BMI from 16.0 to 18.5kg/m². Therefore three BMI groups were defined: women below 21kg/m², men above 25kg/m², and mixed average in-between (21<BMI<25kg/m²). Within each group, there were six subjects of different statures. For each subject, fifty-four anthropometric measurements such as height, thoracic axillary width, thigh circumference, were available for building the subject-specific manikins. Meanwhile, bi-planar X-rays acquisitions (face and profile) from the low dose biplane X-rays device EOSTM (Biospace Instruments, Paris, France) of these subjects in a standing posture had also been collected with the approval obtained from the ethical committee of Paris Saint-Antoine (approval No. 02547). Face and profile views were obtained simultaneously in a calibrated environment (Dubousset et al., 2010; Deschênes et al.,

2010). Subjects were asked to stand in a natural up-right position and hold their breath during the scan. Elbows were slightly raised and the hands gently touched the cheeks.

A specific software package was developed to create 3D reconstructions of bones from the bi-planar radiographs (Dubousset et al., 2010). The 3D bony reconstructions of the spine of each subject including the C3 to L5 vertebrae from EOS acquisitions had been obtained in Bertrand et al. (2006) using a method described in Pomero et al. (2004). For the purpose of this study, we added the 3D reconstructions of the femurs using the method described in Chaibi et al. (2011). EOS showed to be a golden standard to locate the human joint centers (Pillet et al., 2014). Moreover, the skin contour is also visible on both radiographs and data of both external body shape and internal skeleton is thus available.

2.2. Digital manikin generation and postural adjustment

Both HB and RAMSIS, have a module for generating manikins from external anthropometric dimensions. For HB, up to 70 anthropometric measurements such as stature, sitting height, weight, etc. can be input for creating a manikin. In practice, not all required anthropometric measures are available. The missing parameters are automatically estimated from a chosen anthropometric database. A similar procedure can be found in RAMSIS which uses 22 anthropometric dimensions. The anthropometric measures used for generating subject specific HB and RAMSIS manikins in the present study are listed in Table 1. One can see that quite different input parameters are used for these two DHM tools. Most of the body dimensions were manually measured in Bertrand et al. (2006), a few additional measurements were added from the volunteers' EOS radiographs for the purpose of the present study.

Table 1

Each manikin has to be positioned in the same way as the subject scanned in EOS for comparison purposes. For this, the generated subject specific manikins were exported into a customised DHM software tool (named 'RPx'), which could also import EOS radiographic images. Once a digital manikin and its corresponding two radiographic images were imported in RPx, the manikin posture was manually adjusted so as to match the manikin's contour with the subject's skin surface (Figure 1) (see Wang et al., 2005 and Seitz et al., 2000 for a description of the matching method). The operators performing manual superposition were asked to position the pelvis at first and then the upper and lower bodies. As the external body

shape especially at the belly may be quite variable because of the presence of soft tissue, they were instructed to favour the fitting of the dorsal and neck area for the upper body. The operators were asked to adjust the manikin's back profile to match the subject's torso profile in the sagittal plane. Due to limited space of the EOS cabin, the belly of overweight subjects was often cut on the radiographs. In order to avoid the temptation of adjusting the manikin's posture based on the skeleton, the internal linkage of the manikin was coloured in the same colour as the EOS radiographic grey images. All operators were instructed not to refer to the manikins' skeleton during posture adjustment.

Figure 1

2.3. Parameters for comparison between generated subject specific manikins and real subjects

As generated subject specific manikins contain both external body shape and internal skeleton represented by a linkage of joint centers, different parameters are defined and listed in Table 2 for comparison purpose.

For joint centers, RAMSIS has a simplified spine with only seven joints approximately approaching the locations of S2/S3 (GLK), L4/L5 (GLL), T12/L1 (GBL), T8/T9 (GBB), T4/T5 (GHB), C4/C5 (GHH), C1/head (GKH), while Human Builder includes a full representation of the thoracic and lumbar spine. Six joints were selected: knee, hip, C1/head, T4/T5, T8/T9 and T12/L1. They were compared in a global coordinate system from the EOS acquisitions taking into account the orientation of the subject:

Origin: The midpoint between the right (Ac_r) and left (Ac_l) pelvis acetabulum centers

Z: The vertical direction pointing upwards given by EOS system

X: The line perpendicular to the frontal plane containing Ac_r and Ac_l, pointing anteriorly.

Y: The common line perpendicular to Z- and X-axis, pointing to the left.

Positions of the right and left hip and knee joints were pooled together with y coordinates of the right limb being mirrored with respect to the sagittal plane of symmetry. In addition to these six joint positions, distances between knee and hip joint centers (femoral length), between two hip joint centers (hip width), as well as the sum of the distances between these spine joint centers (spine length) were calculated.

Apart from segment lengths, most of external anthropometric dimensions used for generating a manikin are posture dependent. Moreover, they often require the identification of body landmarks (acromion, bust point, navel etc.), which are not represented on the manikins. This makes it difficult even impossible to extract most of anthropometric dimensions that are used for generating manikins. In the present study, a few external measurements were compared and are listed in Table 2. Stature, waist depth and breadth and chest depth were manually measured from both HB and RAMSIS generated manikins from the adjusted EOS standing posture. Standard standing and sitting postures corresponding to those for anthropometric measurements for both HB and RAMSIS were also used for checking if stature, buttock-knee length, and sitting height of generated manikins corresponded to real subjects' anthropometric dimensions. Individual differences in posture were not considered.

Table 2

2.4. Intra and inter operator variability in joint center location

Once a manikin is generated from external anthropometric dimensions, the quality of the superposition of a manikin over its corresponding EOS X-ray images, i.e. joint location, was operator dependent in RPx. To estimate associated uncertainty, three operators participated in the study for an assessment of intra and inter observer variability. One operator was familiar with the procedure of manikin – images matching procedure, called experienced operator. Two others never used RPx before and were trained by the experienced operator. The training consisted in a demonstration and a trial with the assistance of the experienced operator. Four subjects were selected from the three BMI groups (two below 21kg/m², one medium, and one above 25kg/m²) of different statures from 1.58m to 1.89m. The experienced operator performed postural adjustment three times for these 4 subjects, while two other operators did only once. Three indicators were defined to measure the intra operator variability in a joint center location:

- 1) The average of the four mean distances between three observations (n=3) and their mean for a same operator over the four selected subjects (m=4):

$$D_1 = \frac{1}{m} \times \frac{1}{n} \times \sum_{i=1}^m \sum_{j=1}^n \sqrt{(x_{ij} - \bar{x}_i)^2 + (y_{ij} - \bar{y}_i)^2 + (z_{ij} - \bar{z}_i)^2}$$

where (x_{ij}, y_{ij}, z_{ij}) is the joint position of the subject i for the repetition j and $(\bar{x}_i, \bar{y}_i, \bar{z}_i)$ the mean position from three repetitions.

- 2) The average of the four maximum distances (D_2) between three observations ($n=3$) and their mean for a same operator over the four selected subjects ($m=4$):

$$D_2 = \frac{1}{m} \times \sum_{i=1}^m \max_j \left(\sqrt{(x_{ij} - \bar{x}_i)^2 + (y_{ij} - \bar{y}_i)^2 + (z_{ij} - \bar{z}_i)^2} \right)$$

- 3) The average of the four maximum distances (D_3) between three observations ($n=3$) for a same operator over the four selected subjects ($m=4$):

$$D_3 = \frac{1}{m} \sum_{i=1}^m Dis_{i,max}$$

where $Dis_{i,max}$ is the maximum distance between the joint locations from three observations for the subject i .

For the inter operator variability, the results from the first trial of the experienced operator were compared with two other operators. The corresponding indicators were calculated with three operators ($n=3$) for the four selected subjects ($m=4$).

2.5. Statistical analysis

In addition to means and standard deviation of the differences in the parameters defined in Table 2 between generated manikins and corresponding subjects, the effect of BMI was studied with a non-parametric Kruskal-Wallis test. When the Kruskal-Wallis test showed a significant difference between the three BMI groups, a Wilcoxon rank sum test was performed to test which group was significantly different from the others. A paired Student's T-test was performed to compare the differences between RAMSIS and Human Builder manikins.

3. Results

3.1. *External parameters*

Differences in the seven external anthropometric dimensions between generated manikins and real subjects are presented in Table 3. Stature, sitting height, buttock-knee length and chest depth had been used when generating RAMSIS manikins. They showed an error smaller than $6.4\pm 14.1\text{mm}$ whereas waist depth and width, which had been automatically estimated, showed a larger error of $25.2\pm 21.8\text{mm}$ on average. The measures used for generating HB manikins such as chest depth and standard stature showed an error smaller than $8.3\pm 9.0\text{mm}$ on average while the measures that were automatically estimated, such as sitting height, buttock-knee length, waist depth and width, showed larger errors up to $35.0\pm 21.0\text{mm}$. The difference in the stature obtained from the standing posture adopted in EOS was $8.3\pm 9.0\text{mm}$ for HB, slightly higher than $4.5\pm 2.0\text{mm}$ from the standard standing posture. A higher difference was observed for RAMSIS between the two standing postures: the error from the EOS standing position was $-37.5\pm 8.5\text{mm}$ versus $-4.4\pm 5.0\text{mm}$ from the standard standing posture.

Table 3

3.2. *Joint center*

3.2.1. *Intra and inter variability*

The three indicators of the intra and inter operator variability in joints center location after manual postural adjustment is given in Table 4. For intra operator variability, the maximum distance between three repetitions (D_3) was less than 11.3mm for HB, whereas it was higher for RAMSIS with the highest distance of 17.1mm for the knee joint. For inter operator variability, higher differences in D_3 were again observed for RAMSIS with the highest distance of 32.1mm for T4/T5.

Table 4

3.2.2. *Joint center location*

The differences in the location of the six selected joints between generated manikins and the corresponding subjects are summarized in Table 5 and Table 6. As differences in spine joint centers location in the lateral direction (y) were smaller than $1.5\pm 9.5\text{mm}$, only the differences

in x and z are presented in Table 5. Errors in hip lateral location in y axis can be estimated by hip width. Hip width, spine length and femoral length are given in Table 6.

Table 5 and Table 6

Significant differences in the location of knee joint, T4/T5, T8/T9 and C1/head were found between both manikins ($p < 0.05$).

For HB, the average error in distance was 27.6 ± 12.9 mm for all joints from all subjects. Hip and spine joints tended to shift in an opposite posterior-anterior direction (x). The generated manikins had a hip joint positioned posteriorly by -14.3 ± 9.7 mm on average behind the femoral head center, whereas the spine joints T4/T5, T8/T9, T12/L1, C1/head were shifted anteriorly by 13.6 ± 15.8 , 18.2 ± 12.4 , 17.3 ± 9.4 , and 10.4 ± 12.9 mm respectively. Knee joint center was located lower than the center of the two epicondyles by -38.4 ± 11.8 mm on average. Regarding the BMI effect, a significant difference ($p < 0.05$) was found for the hip joint center between the group above 25 kg/m^2 and the two others.

For RAMSIS, differences in joint centers between manikins and corresponding subjects were found with an average distance of 38.3 ± 16.5 mm for all joints and all subjects. Hip joint was shifted upwards by 39.5 ± 16.2 mm on average, whereas there was a downward shift for the four spine joints with the highest shift of -32.7 ± 12.4 mm for T8/T9 joint. T4/T5 was actually close to T6/T7; T8/T9 at the height of T10 and T12/L1 at the height of L1/L2. Knee joint were also shifted upwards by 17.7 ± 11.4 mm.

Regarding the distances measured between joint centers, a significant effect of BMI group on hip width was found for both HB and RAMSIS manikins. Hip width by HB was too large for the group above 25 kg/m^2 , while it was too narrow for the group below 21 kg/m^2 by RAMSIS. For spine length, RAMSIS tended to generate manikins with a spine shorter than real subjects by 44.5 ± 14.9 mm on average, in agreement of the observation on the error in hip and spine joint center locations. Femoral length was systematically too long by 29.9 ± 24.4 mm and 22.0 ± 16.9 mm for HB and RAMSIS.

4. Discussion

In this study, manikins generated by RAMSIS and HB were compared with 18 variously sized females and males divided into three BMI groups. The locations of knee, hip and four spine joint centers as well as seven external anthropometric dimensions were compared. The main observations can be summarized as follows:

- Apart from waist depth and width, both HB and RAMSIS manikins were correctly generated with respect to stature, sitting height, buttock-knee length and chest depth.
- For RAMSIS manikins, hip joint center was systematically displaced by 39.5mm upwards (in z-axis) on average while four other spine joints were shifted downwards by up to -32.7mm for T8/T9. In addition, spine length (sum of distances between joints) was shortened by -44.5 mm while femoral length was too long by 22.0mm.
- For HB manikins, the thoracic spine joints T4/T5, T8/T9 and T12/L1 were systematically shifted anteriorly by 16.4 mm on average while hip joints were shifted posteriorly by -14.3mm. Femoral length was too long by 29.9mm.
- An effect of BMI was mainly found for hip joint center in three directions for HB and only in lateral direction (y-axis) for RAMSIS.

These observations suggest that the estimation of joint centers (including spine, hip and knee joints) from external anthropometric parameters could be improved for both manikins. The significantly lower differences in spine joint centers location for HB compared to RAMSIS may probably be explained by the fact that RAMSIS has a more simplified spine linkage representation with only 7 joints, while HB has a full representation of 12 thoracic and 5 lumbar joints. In addition it is interesting to see that the error in the stature measured from the standard standing was quite small (<10mm) for both RAMSIS and HB. But when using the standing posture adopted in the EOS cabin, RAMSIS manikins were shortened on average by 37.5mm while only a slightly higher error but less than 10mm was observed for HB. This was not due to the differences in the inputs when generating HB and RAMSIS (Table 2), because no significant difference between HB and RAMSIS was found for the three main anthropometric lengths (stature, sitting height and buttock-knee length) used for comparison (Table 3). These results suggest that a better accuracy of the spine curvature representation (including spine joint centers location and the number of spine joints) could improve the manikins' ability to reproduce the position of the internal skeleton from external body shape. Indeed when superimposing a manikin with EOS X-ray images, the operators were asked to match the dorsal profile in priority at the expense of possibly mismatching of the frontal profile. With such an instruction, the operators had to adjust joint angles to respect the natural lordosis and kyphosis of the subjects' dorsal profile. Due to its simplified representation and

too-flat shape of the back profile, RAMSIS spine model was excessively shortened and hip joint centers were pulled upwards during the matching onto subjects' back profile. A different instruction may have reduced the differences found between both manikins. Indeed, an alternative matching method could be to position the knees at first and then adjust hip and spine angles so that the head reach to the right height. This alternative method is illustrated in Figure 2 with RAMSIS for a subject. As expected, the errors in z for the hip and knee joints were much reduced compared to the back profile matching method, while an inconsistent lower back profile was obtained and the errors affecting spine joint centers were even bigger. Aware of the fact that the errors in joint centers are dependent on the manikin-EOS images matching method, the differences in hip width, spine length and femoral length, which are independent of matching method, are also provided in Table 6. The error in the spine length for RAMSIS manikins was 44.5mm on average much higher than for HB. Using this alternative matching method will not change the main conclusion about the importance of a more detailed representation of the spine. In the case of the RAMSIS manikins, it should be noted that the joints of the spine model are not intended to be accurately positioned at their anatomical locations (Reed et al., 1999).

In this study, the possible effect of BMI was also investigated. Hip joint center location for both HB and RAMSIS was subject to BMI effect. For RAMSIS, stature in a standard posture was significantly less accurate for the lowest BMI group compared to the highest BMI group. Otherwise no significant effect was found for most of the other parameters studied: a high difference was found for two waist dimensions irrespective of BMI groups, relatively large errors in z direction of the six joint centers for RAMSIS were not affected by the BMI group either.

The standard deviations (SD) of the errors of joint centers in x and z with respect to their mean values were high in general, because signed errors were used instead of absolute differences. An average value of zero means that errors are evenly distributed in both directions of an axis. An average value higher than SD suggests a systematic shift in one direction. This was the case particularly for the knee of HB manikins in z (-38.4 ± 11.8 mm from all subjects, systematically too low). For RAMSIS manikins, hip was systematically located too high (39.5 ± 16.2 mm) with too low spine joints (Table 5).

As the postural adjustment was operator dependent, the methodology of manikin-X-ray images matching was evaluated by measuring the inter and intra operator variability in joints location using three indicators D1, D2, D3 (Table 4). The mean errors in joint centers

between manikins and real subjects were higher than D3, the maximum difference between three repetitions or between three operators. Only RAMSIS's knee joint and HB's C1/head errors were slightly smaller than D3.

The first limitation of this study is that the inter operator variability was more than twice as high as the intra operator variability. Such variability among operators might be due the subjective appreciation required when matching the manikins' contour on the subjects' radiographs. Another limitation is that X-rays images were cut at the calf level. This implies that the adjustment of manikin's posture in the vertical direction was mainly guided by the position of subjects' head and back profile. This may induce an excessive displacement of the manikins upwards and excessive errors in the underlying joints position in the vertical direction (z). Matching the position of the knees and the head could improve the knee and hip location, but leads to an inconsistent spine profile.

It should be noted that the inaccuracy in joint location of a human model has almost no consequence on most of ergonomics assessments such as vision, fit, clearance and reach, which are mainly based on postural analysis. However, inaccuracy in joint location mainly impacts joint load and muscle forces. Differences between both manikins showed that a more realistic model led to more accuracy in joint location and would be more appropriate for biomechanical analysis. This is particularly true in the case that several different human models are required implying data exchange between them. As already expressed for the need of standardization of human models by Paul and Wischniewski (2012), a more explicit description in joint center definition of current manikins is required. As joint centers for posture or motion analysis is usually defined from external body landmarks (e.g. Reed et al, 1999), the information about body landmarks as well as their relationships is also required for defining more realistic human models.

For the first time, the external body shape and the internal skeleton of a subject in a standing posture were used simultaneously for the evaluation of current digital human manikins. With such an approach this study opens the way to further research on the relationship between external body parameters (landmarks, measures etc.) and internal skeleton in order to reduce the errors in joints location and improve the realism of current digital human manikins.

5. Conclusion

Subject specific manikins generated by RAMSIS and Human Builder, two digital human modeling systems widely used in industry, were assessed with help of EOS X-ray images in terms of both external anthropometric dimensions and internal joint locations. Results clearly show that both could correctly reproduce external anthropometric dimensions while large errors in internal joints centers location were found. Differences between both manikins also showed that a more realistic kinematic linkage led to more accuracy in joint location. This study opens the way to further research on the relationship between the external body geometry and internal skeleton in order to improve the realism of current digital human manikins' skeletal model especially for a biomechanical analysis requiring information of joint load and muscle force estimation.

Acknowledgement

The clinical data used in this study were provided by the LBM, Arts et Métiers ParisTech, Paris, collected within the HUMOS 2 project (G3RD-CT-2002-00803) funded by the European Community, the French Ministry of Research (FNS) and the Ile de France region (SESAME N°E1424). The authors would like to thank Dr. Hans-Joachim Wirsching of Human Solutions for his technical assistance.

References

- Bertrand, S., Kojadinovic, I., Skalli, W., and Mitton, D. 2009. Estimation of External and Internal Human Body Dimensions From Few External Measurements. *Journal of Musculoskeletal Research*, 12(04), 191–204.
- Bonin, D., Wischniewski, S., Wirsching, H, J., Upmann, A., Rausch, and J., Paul, G. 2014. Exchanging data between Digital Human Modelling systems : a review of data formats. In 3rd International Digital Human Modeling Symposium, AIST, Tokyo.
- Bubb, H., and Fritzsche, F. 2009. A scientific Perspective of Digital Human Models: Past, Present, and Future, in *Handbook of Digital Human Modeling*. Duffy, V. G., Ed., CRC Press, Taylor & Francis Group, Boca Raton, Florida, 3, 1-30.
- Chaffin, D. B. 1997. Development of Computerized Human Static Strength Simulation Model for Job Design. *Human Factors and Ergonomics in Manufacturing*, 7(4), 305-322.
- Chaibi, Y., Cresson, T., Aubert, B., Hausselle, J., Neyret, P., Hauger, O., de Guise J. A., and Skalli, W. 2011. Fast 3D Reconstruction of the Lower Limb Using a Parametric Model and Statistical Inferences and Clinical Measurements Calculation from Biplanar X-Rays. *Computer Methods in Biomechanics and Biomedical Engineering*, 15(5), 457–66.
- Damsgaard, M., Rasmussen, J., Christensen, S.T., Surma, E., and de Zee, M. 2006. Analysis of Musculoskeletal Systems in the Anybody Modeling System. *Simulation Modelling Practice and Theory*, 14(8), 1100–1111.
- Delp, S.L. and Maloney, W. 1993. Effect of Hip Center Location on the Moment- Generating Capacity of the Muscles. *Journal of Biomechanics*, 26(4-5), 485-499.
- Deschênes, S., Charron G., Beaudoin, G., Labelle H., Dubois J., Miron M.C., and Parent S. 2010. Diagnostic Imaging of Spinal Deformities : Reducing Patients Radiation Dose With a New Slot-Scanning X-ray Imager. *SPINE*, 35(9), 989-994.
- Dubousset J., Charpak G., Skalli W., Deguise J. and Kalifa G. 2010. EOS: A New Imaging System With Low Dose Radiation in Standing Position for Spine and Bone & Joint Disorders. *Journal of Musculoskeletal Research*, 13(1), 1-12.
- Paul, G., and Wischniewski S. 2012. Standardisation of Digital Human Models, *Ergonomics*, 55(9), 1115-1118.
- Grujicic, M., Pandurangan, B., Xie, X., Gramopadhye, A. K., Wagner, D., and Ozen, M. 2010. Musculoskeletal Computational Analysis of the Influence of Car-seat Design/Adjustments on Long-Distance Driving Fatigue. *International Journal of Industrial Ergonomics*, 40(3), 345-355.
- Pillet H., Sangeux M., Haussella J., and El Rachkidia R. 2013. A Reference Method for the Evaluation of Femoral Head Joint Ceter Location Technique Based on External Markers. *Gait & Posture*, 39(1), 655-658

- Pomero, V., Mitton, D., Laporte, S., de Guise, J. A. and Skalli, W. 2004. Fast Accurate Stereoradiographic 3D-Reconstruction of the Spine Using a Combined Geometric and Statistic Model. *Clinical Biomechanics*, 19, 240–247.
- Rebiffe, R., Guillien, J., and Pasquet, P. 1982. Enquête anthropométrique sur les conducteurs français. Laboratoire de physiologie et de biomécanique de l'association Peugeot-Renault, France.
- Reed, M.P., Manary, M. A., and Schneider, L.W. 1999. Methods for Measuring and Representing Automobile Occupant Posture. Technical Paper 990959. Warrendale, PA: Society of Automotive Engineers, Inc.
- Seitz, T., Balzulat, J., and Bubb, H. 2000. Anthropometry and Measurement of Posture and Motion. *International Journal of Industrial Ergonomics*, 25, 447-453.
- Siefert, A., Pankoke, S., Wölfel, H.-P. 2008. Virtual Optimization of Car Passenger Seats: Simulation of Static and Dynamic Effects on Drivers' Seating Comfort. *International Journal of Industrial Ergonomics*, 38, 410–424.
- Snyder, R.G., Chaffin, D. B. and Schutz, R. K. 1972. Link System of the Human Torso. Aerospace Medical Research Laboratory, Wright-Patterson AFB, Ohio. AMRL-TR-71-88.
- Wang, X., Chevalot, N., Monnier, G., Ausejo, S. et al. 2005. Validation of a Model-based Motion Reconstruction Method Developed in the REALMAN Project. SAE Technical Paper 2005-01-2743.
- You, H., Ryu, T. 2005. Development of a Hierarchical Estimation Method for Anthropometric Variables. *International Journal of Industrial Ergonomics*, 35, 331–343.
- Zehner, G. F., Oudenhuijzen, A., and Hudson, J. 2009. A Verification and Validation of Human Modeling Systems, in *Handbook of Digital Human Modeling*. Duffy, V. G., Ed., CRC Press, Taylor & Francis Group, Boca Raton, Florida, 3, 1-30.

Tables

Table 1: List of the input parameters to generate Human Builder and RAMSIS manikins. The parameters with EOS were measured indirectly from EOS radiographs. All others were measured manually obtained on the volunteers.

Parameter name	Parameters definition	HB (15)	RAMSIS (18)
Stature	Distance from a standing surface to the top of the head	x	x
Weight		x	x
Gender		x	x
Acromial height	Distance between the standing surface and the acromion	x	
Buttock depth	Horizontal depth of the torso at the level of the maximum protrusion of the right buttock	x	
Hip breadth	Distance between the hips at the level of the lateral buttock landmarks.	x	
Knee height	Distance between the standing surface and the center of the knee at the midpatella landmark	x	
Foot length	Distance between the tip of the longest toe and the back of the heel of the standing foot	x	
Abdominal extension depth	Distance between the anterior point of the abdomen and the back at the same level	x	
Chest depth (EOS)	Distance between the chest at the level of the bust point on women and the nipple on men, and the back at the same level	x	x (at the level of xiphoid)
Waist breadth (sitting)	Horizontal breadth of the waist at the level of the center of the navel (omphalion)	x	
Chest breadth	Maximum horizontal breadth of chest at the level of the bust point/thelion	x	
Upper arm length	Distance between the acromion and the olecranon landmark at the bottom of the elbow flexed to 90 degrees.	x	x
Forearm length	Distance between the radiale landmark on the elbow and the stylium landmark on the wrist	x	
Trochanterion height	Vertical distance between the standing surface and the trochanterion landmark of the hip	x	
Sitting height	Distance in the vertical plane between the top of the head and seat horizontal surface		x

Buttock-knee length	Distance from the most prominent point in the buttocks region to the most prominent point of the right knee at the patella or immediately below the patella.	x
Maximum thigh circumference	Maximum circumference of the thigh orthogonally to the leg axis.	x
Maximum lower leg circumference	Maximum circumference of the lower leg orthogonally to the leg axis	x
Maximum upper arm circumference	Horizontal circumference of the relaxed right upper arm at the level of the maximum convexity of the biceps.	x
Maximum forearm circumference	Horizontal circumference of the right forearm at the point of maximum prominence slightly distal of the elbow joint.	x
Head width	Distance of the two points at both sides of the head which are most prominent in a frontal plane.	x
Head height (EOS)	Distance from the highest point of the head in the median plane to the lowermost point of the lower jaw in the median plane.	x
Foot length	Distance between the tip of the longest toe and the back of the heel of the standing foot	x
Foot breadth	Distance from the medially most prominent point of the first metatarsal bone to the laterally most prominent point of the fifth metatarsal bone.	x
Seat height	Distance from the sitting plane to the highest point of the head in the median plane	x
Pelvis width	Straight distance of the two laterally most prominent points at the outer edge of the ilium	x
Head depth	Distance from the glabella to the opisthocranium.	x

Table 2. List of the parameters used for comparing generated HB and RAMSIS manikins with EOS reconstructions.

N°	Parameter	Definition
1	C1/head	Top of the odontoid process
2	T4/T5	Middle point of the segment joining the barycenter of T4 under plate and T5 upper plate (Snyder et al. 1972)
3	T8/T9	Middle point of the segment joining the barycenter of T8 under plate and T9 upper plate (Snyder et al. 1972)
4	T12/L1	Middle point of the segment joining the barycenter of T12 under plate and L1 upper plate (Snyder et al. 1972)
5	HJC_r	Right femoral head center(Chaibi et al., 2012)
6	HJC_l	Left femoral head center(Chaibi et al., 2012)
7	Knee joint center	Middle point of the axis joining the centers of two spheres fitted inside the femoral epicondyles
8	Hip width	Distance between the two hip joint centers
9	Spine length	Sum of the distances between (HJC_r+HJC_l)/2, C1/head, T4/T5, T8/T9, T12/L1, L4/L5
10	Femoral length	Distance between the hip joint centers and the knee joint centers
11	Stature	Cf. Table 1
12	Buttock-Knee length	Cf. Table 1
13	Sitting height	Cf. Table 1
14	Waist depth	Distance between the front and back of the waist at the level of the center of the navel
15	Waist width	Waist breadth at the level of the center of the navel
16	Chest depth	Cf. Table 1

Table 3. Means and standard deviations (\pm SD) of the differences in external parameters between HB and RAMSIS manikins and subjects' measurements (reference) in mm. P-values of the tests for the effect of BMI by a multi-factor Kruskal-Wallis test are indicated.

Group	EOS standing								Standard standing and sitting					
	Stature		Waist depth		Waist width		Chest depth		Stature		Buttock-Knee length		Sitting height	
	HB [†]	RAMSIS [†]	HB [†]	RAMSIS [†]	HB [†]	RAMSIS [†]	HB	RAMSIS	HB	RAMSIS	HB [†]	RAMSIS	HB [†]	RAMSIS
BMI<21	-1.7 \pm 10.9	-37.5 \pm 4.0	-19.8 \pm 8.2	11.5 \pm 14.4	38.4 \pm 16.7	27.6 \pm 17.6	-0.5 \pm 0.5	-8.3 \pm 9.7	2.0 \pm 2.4	-9.7 \pm 0.8	2.8 \pm 15.8	4.0 \pm 6.6	8.5 \pm 17.6	0.6 \pm 19.2
21<BMI<25	9.7 \pm 4.4	-35.6 \pm 12.6	-24.3 \pm 18.1	10.8 \pm 24.4	32.5 \pm 24.2	29.5 \pm 14.1	-2.4 \pm 1.5	2.1 \pm 10.9	4.8 \pm 3.7	-3.1 \pm 5.2	32.8 \pm 21.3	6.1 \pm 10.9	-7.8 \pm 10.2	-5.2 \pm 1.6
BMI>25	11.6 \pm 3.4	-39.5 \pm 8.0	-26.05 \pm 18.8	21.5 \pm 21.4	34.0 \pm 24.0	50.1 \pm 29.4	-1.9 \pm 2.5	-1.4 \pm 27.6	6.6 \pm 2.7	-0.3 \pm 0.4	19.02 \pm 29.9	9.0 \pm 22.3	1.4 \pm 31.9	-4.1 \pm 0.0
Total	8.3 \pm 9.0	-37.5 \pm 8.5	-23.4 \pm 14.6	14.6 \pm 20.9	35.0 \pm 21.0	35.7 \pm 22.7	-1.6 \pm 1.8	-2.5 \pm 15.7	4.5 \pm 2.0	-4.4 \pm 5.0*	18.2 \pm 25.1	6.4 \pm 14.1	0.7 \pm 23.6	-2.9 \pm 10.8

* $p < 0.05$, [†] Dimension not used for generating manikin.

Table 4: Intra and inter operator variability in joint center in mm.

			Knee	Hip	C1/head	T4/T5	T8/T9	T12/L1	All
HB	Intra	D₁	4.8	3.3	3.8	2.8	2.7	2.3	3.3±0.9
		D₂	6.8	4.6	4.9	3.8	3.8	3.5	4.6±1.2
		D₃	11.3	7.4	8.9	7.0	6.7	5.6	7.8±2.0
	Inter	D₁	10.6	8.7	10.1	7.2	6.4	5.8	8.1±2.0
		D₂	14.6	11.5	12.9	9.3	8.9	7.8	10.8±2.6
		D₃	25.1	18.8	23.6	15.8	16.2	13.9	18.9±4.5
RAMSIS	Intra	D₁	7.8	5.7	6.6	5.2	5.2	5.3	6.0±1.0
		D₂	10.0	7.8	9.1	7.1	6.8	7.4	8.0±1.3
		D₃	17.1	13.0	16.5	11.7	11.9	12.9	13.9±2.4
	Inter	D₁	11.4	11.9	10.7	15.4	12.4	8.8	11.8±2.2
		D₂	14.9	15.7	14.4	19.9	15.6	11.3	15.3±2.8
		D₃	27.0	26.6	24.0	32.1	15.9	19.9	24.3±5.7

Table 5: Means and standard deviations (\pm SD) of the differences (in mm) of the selected joint locations in anterior-posterior (Δx) and upwards-downwards (Δz) directions between HB and RAMSIS manikins and corresponding subjects (reference) by BMI group. The distances (3D) were also calculated. Right and left knees and hips were pooled into a single joint (n=36) with y coordinates of the right side being mirrored with respect to the sagittal plane. Effects of BMI group by a multi-factor Kruskal-Wallis test are indicated.

	Knee		Hip		T4/T5		T8/T9		T12/L1		C1/head		ALL joints		
	HB	RAMSIS	HB	RAMSIS	HB	RAMSIS	HB	RAMSIS	HB	RAMSIS	HB	RAMSIS	HB	RAMSIS	
BMI<21	Δx	6.4 \pm 12.7	17.9 \pm 9.4	-10.4 \pm 6.6	-9.0 \pm 8.2	11.1 \pm 9.2	-28.7 \pm 15.5	17.7 \pm 9.0	-12.9 \pm 11.0	19.8 \pm 6.6	6.3 \pm 12.5	8.3 \pm 15.2	-8.9 \pm 10.5	8.8 \pm 15.2	-5.9 \pm 18.6
	Δz	-35.7 \pm 12.4	13.2 \pm 9.9	-17.5 \pm 6.4	41.2 \pm 8.8	2.6 \pm 6.8	-27.5 \pm 8.7	-15.5 \pm 6.0	-35.5 \pm 9.8	-8.1 \pm 8.1	-34.0 \pm 9.9	-7.7 \pm 3.1	-19.8 \pm 7.2	-17.0 \pm 11.3	-10.4 \pm 31.7
	3D	39.2 \pm 11.2	26.2 \pm 8.6	22.8 \pm 6.3	45.7 \pm 8.8	14.7 \pm 7.6	40.4 \pm 16.6	25.8 \pm 8.1	39.0 \pm 11.5	35.1 \pm 8.7	36.5 \pm 11.1	17.0 \pm 9.0	23.4 \pm 10.5	25.8 \pm 9.9	35.2 \pm 13.2
21<BMI<25	Δx	0.4 \pm 14.3	8.5 \pm 12.44	-10.9 \pm 11.3	-3.5 \pm 9.1	14.8 \pm 23.8	-47.7 \pm 9.9	18.3 \pm 16.3	-19.4 \pm 10.0	16.1 \pm 13.6	-0.9 \pm 11.6	17.2 \pm 10.4	-12.8 \pm 16.5	6.6 \pm 14.8	-12.3 \pm 20.9
	Δz	-35.1 \pm 12.9	20.5 \pm 12.6	3.6 \pm 11.6	38.0 \pm 15.9	4.2 \pm 14.2	-25.3 \pm 10.1	-5.6 \pm 15.9	-30.1 \pm 12.4	-10.0 \pm 22.0	-28.8 \pm 18.5	-11.3 \pm 9.2	-20.8 \pm 7.7	-10.2 \pm 18.0	-10.7 \pm 35.0
	3D	39.0 \pm 12.4	27.7 \pm 10.9	21.1 \pm 8.7	40.5 \pm 16.1	22.2 \pm 22.7	55.5 \pm 8.9	23.0 \pm 19.5	38.8 \pm 8.8	27.0 \pm 17.2	33.8 \pm 14.5	22.7 \pm 10.6	27.5 \pm 13.8	24.9 \pm 12.4	39.8 \pm 17.6
BMI>25	Δx	-11.8 \pm 12.1	5.7 \pm 7.5	-21.7 \pm 6.4	-7.6 \pm 7.6	14.9 \pm 13.6	-54.9 \pm 12.0	18.5 \pm 13.3	-24.3 \pm 10.7	16.1 \pm 7.9	2.2 \pm 11.4	5.8 \pm 11.9	-21.1 \pm 5.6	3.6 \pm 19.9	-15.8 \pm 20.0
	Δz	-44.6 \pm 9.1	19.4 \pm 12.0	-13.1 \pm 31.7	39.4 \pm 22.4	7.2 \pm 10.3	-26.7 \pm 16.7	-5.1 \pm 10.2	-32.7 \pm 16.0	-12.5 \pm 13.7	-31.7 \pm 20.1	-15.4 \pm 9.2	-26.3 \pm 9.7	-16.3 \pm 22.1	-9.8 \pm 34.6
	3D	48.6 \pm 9.8	22.9 \pm 10.7	40.1 \pm 18.6	42.0 \pm 21.6	23.7 \pm 5.8	63.9 \pm 13.8	24.7 \pm 9.9	43.9 \pm 13.2	25.7 \pm 8.9	36.3 \pm 17.0	21.9 \pm 4.9	35.5 \pm 8.4	32.1 \pm 14.6	39.7 \pm 18.4
subjects	Δx	-1.6 \pm 16.7	10.7 \pm 12.4	-14.3 \pm 9.7*	-6.7 \pm 8.4	13.6 \pm 15.8	-43.8 \pm 16.5*	18.2 \pm 12.4	-18.9 \pm 11.0	17.3 \pm 9.4	3.1 \pm 11.4	10.4 \pm 12.9	-14.3 \pm 12.2	6.3 \pm 16.7	-11.3 \pm 20.0
	Δz	-38.4 \pm 11.8	17.7 \pm 11.4	-10.0 \pm 21.4*	39.5 \pm 16.2	4.6 \pm 10.4	-26.5 \pm 11.6	-8.7 \pm 11.8	-32.7 \pm 12.4	-16.8 \pm 16.9	-31.5 \pm 15.9	-11.5 \pm 7.9	-22.3 \pm 8.3	-14.5 \pm 18.0	-10.3 \pm 33.5
All	3D	42.3 \pm 12.1	25.6 \pm 10.0	28.0 \pm 14.8*	42.7 \pm 16.0	20.2 \pm 14.0	53.3 \pm 16.1*	24.5 \pm 12.7	40.6 \pm 10.9	29.2 \pm 12.3	35.5 \pm 13.6	20.5 \pm 8.4	28.8 \pm 11.7	27.6 \pm 12.9	38.3 \pm 16.5

*p<0.05

Table 6. Means and standard deviations (\pm SD) of the differences in hip width, spine length and femoral length calculated from joint centers between HB and RAMSIS manikins and subjects' measurements (reference) in mm. P-values of the tests for the effect of BMI by a multi-factor Kruskal-Wallis test are indicated.

	Hip width		Spine length		Femoral length	
	HB	RAMSIS	HB	RAMSIS	HB	RAMSIS
BMI<21	-3.4 \pm 9.4	-24.4 \pm 9.9	5.9 \pm 5.6	-47.7 \pm 10.6	16.1 \pm 12.0	25.3 \pm 6.2
21<BMI<25	15.6 \pm 13.5	-15.0 \pm 2.9	-17.7 \pm 21.5	-40.4 \pm 20.6	40.6 \pm 21.0	19.5 \pm 12.4
BMI>25	20.6 \pm 16.5	1.9 \pm 8.7	-11.3 \pm 35.1	-45.5 \pm 13.6	32.9 \pm 32.7	21.3 \pm 27.6
Total	10.9 \pm 16.5*	-12.1 \pm 13.4**	-7.7 \pm 24.8	-44.5 \pm 14.9	29.9 \pm 24.4	22.0 \pm 16.9

p<0.05, *p<0.01

Figures

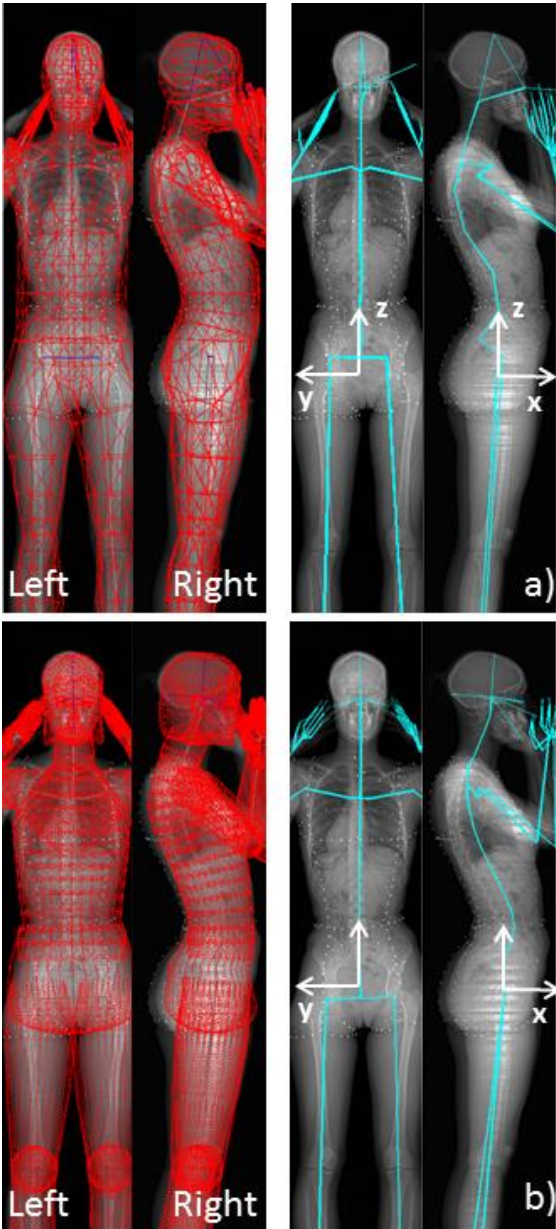


Figure 1. Posture adjustment of a personalized manikin’s external shape upon the visible skin contours of a real subject in the two EOS X-ray images, a) RAMSIS, b) HB

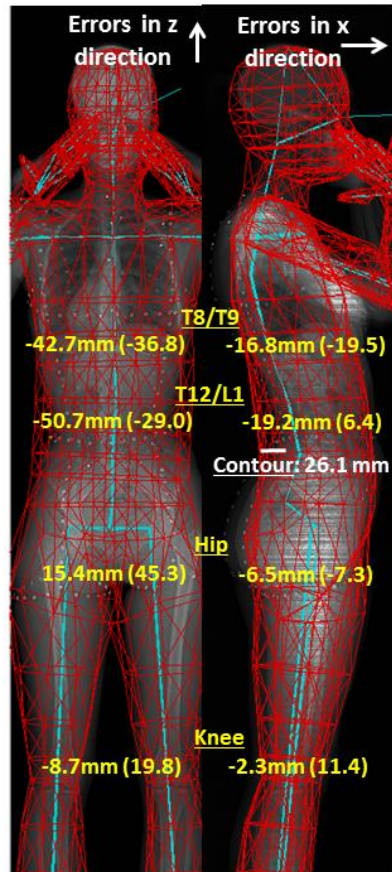


Figure 2. An alternative posture adjustment method of a personalized RAMSIS manikin's external shape upon the contour of the corresponding real subject in the two EOS X-ray images. Knees are positioned at first, then the hip and spine flexion extension angles are adjusted to get the top of the head to the right height. Errors in joint centers in the x and z directions as well as the largest gap in back profile (Contour) are indicated. Errors obtained by the back profile matching method used in the present study are also indicated in brackets.